

Modeling of the Unsteady State Methanol Synthesis at the Level of Catalyst Pellet

IONUT BANU, IOANA STOICA, GHEORGHE BUMBAC, GRIGORE BOZGA*

University Politehnica of Bucharest, Department of Chemical and Biochemical Engineering, 1-7 Polizu Str., 011061, Bucharest, Romania

In a fixed bed of porous catalyst pellets, there are developed two composition and temperature fields, one in the fluid phase and the other one at the level of solid pellets. The objective of this work is to evaluate, by numerical simulation, the unsteady state behavior of a catalyst pellet in typical operating conditions for methanol synthesis reactors. The process kinetics was described by the model published by Graaf et al (1990) and the reaction-diffusion process inside the pellet is based on the Wilke-Bosanquet model. The results showed a short composition and temperature stabilization time, generally below 4 seconds, for a spherical catalyst pellet having typical dimensions for industrial applications.

Keywords: methanol synthesis, catalyst pellet, unsteady-state regime, effectiveness factor

Methanol is one of the most important bulk synthetic organic chemicals manufactured worldwide, with the largest amount (approx. 50 %) used for the manufacture of formaldehyde, while other established applications include synthesis of chloromethanes, amines, acetic acid, and methyl methacrylate [1]. The increased interest for methanol is based also on its use in the production of renewable and cleaner combustibles [2]: synthesis of fuel additives by olefins etherification, production of biodiesel and dimethyl-ether synthesis [3, 4]. There are also well-developed technologies for methanol conversion to olefins and other hydrocarbons, interesting for post-petroleum world period.

The methanol synthesis process is industrially carried out either in cooled multi-tubular reactors or in a series of adiabatic fixed beds, with direct and indirect cooling between the beds [5, 6]. More recent approaches, considered forced unsteady-state processes to synthesize methanol at the pilot plant scale. An experimental study of methanol synthesis in a reverse flow reactor was published by Neophytides and Froment [7]. The same research group published studies regarding the modeling and simulation of reverse flow reactors [8] as well as a STAR network of fixed-bed reactors with periodical change of feed point [9] in methanol synthesis process. These authors aimed slightly better results of unsteady-state operating technologies in comparison with the classical steady-state ones.

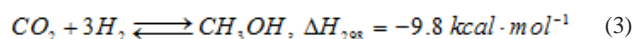
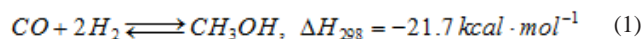
In the analysis of the unsteady state regimes of catalyst beds, there are developed two distinct composition profiles, one inside the flowing gas-phase and the other one inside the catalyst pellet, the last one determining the effective reaction rate. An objective of the process simulation at the level of the pellet is the evaluation of the stabilization time at this level. These are the reasons that make interesting the study of the process at the catalyst level, as component of process simulation at the level of catalytic reactor. At our best knowledge, the only study accounting for the transient regime inside a methanol synthesis catalyst pellet is published by Solsvik and Jakobsen [10], but no detailed information regarding the stabilization time is provided.

The goal of this work is to provide a detailed study of space and time evolutions of concentration and temperature, during transient regimes of a catalyst pellet

in conditions typical for methanol synthesis process in forced unsteady-state regimes.

Mathematical model of the process

The diffusion-reaction process taking place in catalyst pellet was described by the Wilke-Bosanquet model [2, 11]. This model was found to be adequate, giving results close to those predicted by dusty-gas model, when the mass transport occurs by Knudsen and molecular diffusion mechanisms [11]. The reactions commonly considered in methanol production from synthesis gas are CO and CO₂ hydrogenation to methanol and water gas shift reaction [12]:



The rates of these reactions were calculated by using the kinetic model published by Graaf et al (1990) [12], presented in table 1.

Temperature and pressure as operating conditions in process modeling are strictly in the specific intervals established by the gas or vapor phase composition and by the catalyst used in the methanol synthesis.

The mass balance for a chemical species *j* involved in a chemical process taking place inside a spherical catalyst pellet, in unsteady state regime, is expressed by the following equation [8]:

$$\varepsilon_p \frac{\partial C_j}{\partial t} = \frac{1}{r^2} \frac{\partial}{\partial r} (r^2 N_j) - R_j \rho_p \quad (4)$$

Expressing the diffusion flux, *N_j*, by Fick's law, the equation takes the form:

$$\varepsilon_p \frac{\partial C_j}{\partial t} = D_j^{\text{eff}} \left(\frac{\partial^2 C_j}{\partial r^2} + \frac{2}{r} \frac{\partial C_j}{\partial r} \right) - R_j \rho_p \quad (5)$$

The unsteady state heat balance inside the catalyst pellet is expressed by following equation:

$$\rho_p c_s \frac{\partial T}{\partial t} = \frac{\lambda_{\text{eff}}}{r^2} \frac{\partial}{\partial r} \left(r^2 \frac{\partial T}{\partial r} \right) + \sum_{i=1}^3 (-\Delta H_{Ri}) v_{p,i} \rho_p \quad (6)$$

The associated initial and boundary conditions are:

* email: g_bozga@chim.upb.ro

Table 1
RATE EXPRESSIONS AND THE CORRESPONDING KINETIC PARAMETERS

Rate expressions	$v_{p,1} = \frac{k_1 K_{CO} [f_{CO} f_{H_2}^{3/2} - f_{CH_3OH} / (f_{H_2}^{1/2} K_{p1})]}{(1 + K_{CO} f_{CO} + K_{CO_2} f_{CO_2}) [f_{H_2}^{1/2} + (K_{H_2O} / K_{H_2}^{1/2}) f_{H_2O}]}$ $v_{p,2} = \frac{k_2 K_{CO_2} [f_{CO} f_{H_2} - f_{H_2O} f_{CO} / K_{p2}]}{(1 + K_{CO} f_{CO} + K_{CO_2} f_{CO_2}) [f_{H_2}^{1/2} + (K_{H_2O} / K_{H_2}^{1/2}) f_{H_2O}]}$ $v_{p,3} = \frac{k_3 K_{CO_2} [f_{CO_2} f_{H_2}^{3/2} - f_{CH_3OH} f_{H_2O} / (f_{H_2}^{3/2} K_{p3})]}{(1 + K_{CO} f_{CO} + K_{CO_2} f_{CO_2}) [f_{H_2}^{1/2} + (K_{H_2O} / K_{H_2}^{1/2}) f_{H_2O}]}$
Kinetic parameters	$k_1 = 4.89 \cdot 10^7 \cdot \exp\left(\frac{-113000}{R_G T}\right), \text{ mol bar}^{-1.5} \text{ kg}_{cat}^{-1} \text{ s}^{-1}$ $K_{CO} = 2.16 \cdot 10^{-5} \cdot \exp\left(\frac{46800}{R_G T}\right), \text{ bar}^{-1}; \quad K_{CO_2} = 7.05 \cdot 10^{-7} \cdot \exp\left(\frac{61700}{R_G T}\right), \text{ bar}^{-1}$ $\frac{K_{H_2O}}{K_{H_2}^{1/2}} = 6.37 \cdot 10^{-9} \cdot \exp\left(\frac{84000}{R_G T}\right), \text{ bar}^{-1}; \quad \lg K_{p1} = \frac{5139}{T} - 12.621, \quad [K_{p1}] = \text{bar}^{-2}$ $k_2 = 9.64 \cdot 10^{11} \cdot \exp\left(\frac{-152900}{R_G T}\right), \text{ mol bar}^{-1.5} \text{ kg}_{cat}^{-1} \text{ s}^{-1}; \quad \lg K_{p2} = -\frac{2073}{T} + 2.029$ $k_3 = 1.09 \cdot 10^5 \cdot \exp\left(\frac{-87500}{R_G T}\right), \text{ mol bar}^{-1.5} \text{ kg}_{cat}^{-1} \text{ s}^{-1}; \quad K_{p3} = K_{p1} K_{p2}$

In the calculation of the effective diffusion coefficient,

$$t=0, \quad r \in [0, R_p], \quad C_j(r,0) = C_{j0}; \quad T(r,0) = T_0;$$

$$t > 0, \quad r=0, \quad \frac{\partial C_j(0,t)}{\partial r} = 0, \quad \frac{\partial T(0,t)}{\partial r} = 0; \quad r=R_p, \quad C_j(R_p,t) = C_{j,s}, \quad T(R_p,t) = T_s \quad (7)$$

the Knudsen and molecular diffusion mechanisms were considered. The Knudsen diffusion coefficient was evaluated by the relation [13]:

$$D_{K,j} = 9.7 \cdot 10^{-3} \cdot r_{por} \cdot \sqrt{\frac{T}{M_j}} \quad (8)$$

and the binary molecular diffusion coefficients by Fuller relation [14]:

$$D_{ij} = \frac{1.43 \cdot 10^{-7} \cdot T^{1.75}}{P \cdot M_{ij}^{1/2} \cdot [V_i^{1/3} + V_j^{1/3}]^2} \quad ; \quad M_{ij} = 2 \left(\frac{1}{M_i} + \frac{1}{M_j} \right)^{-1} \quad (9)$$

The average diffusion coefficient was evaluated by Bosanquet relation [10]:

$$\frac{1}{\bar{D}_j} = \frac{1}{D_j} + \frac{1}{D_{K,j}} \quad (10)$$

The molecular diffusion coefficient of the species j was determined by Wilke relation [10]:

$$D_j = \frac{1-y_j}{\sum_{i=1, i \neq j}^N \frac{y_i}{D_{ji}}} \quad (11)$$

The effective diffusion coefficient in the porous medium was evaluated using relation. In this relation, the ratio ε / τ was considered as 0.123, value reported by Graaf et al (1990) [12]:

$$D_j^{eff} = \bar{D}_j \frac{\varepsilon}{\tau} \quad (12)$$

The non-ideal behaviour of the gaseous mixture was taken into account by using the Soave-Redlich-Kwong equation of state, as suggested by Graaf et al (1990) [15] and Lommerts et al (2000) [11].

Results and discussions

The unsteady-state mass balance equations were integrated by the method of lines [16]. In this aim the radial coordinate was discretized in a number of equal intervals, Δr , and the spatial derivatives from eqs. (5) and (6) were approximated by finite difference expressions:

$$\frac{\partial \varphi}{\partial r}(k,j) = \frac{\varphi_{k+1,j} - \varphi_{k,j}}{\Delta r}; \quad \frac{\partial^2 \varphi}{\partial r^2}(k,j) = \frac{\varphi_{k+1,j} - 2\varphi_{k,j} + \varphi_{k-1,j}}{\Delta r^2} \quad (13)$$

Thus, it was obtained a system of first order differential equations in respect with the time, which was integrated numerically, obtaining the time evolutions of concentration values in the radial discretization points.

In the integration we used a number of 100 radius discretization intervals. In order to evaluate the accuracy of the integration calculations, it was checked the mass balance for the chemical species on the pellet volume and the simulated process duration:

$$4\pi R_p^2 D_j^{eff} \int_0^{t_f} \frac{\partial C_j(R_p, t)}{\partial r} dt = 4\pi \int_0^{t_f} \int_0^{R_p} r^2 R_j(r, t) dr dt + 4\pi \varepsilon_p \int_0^{R_p} r^2 [C_j(r, t_f) - C_j(r, 0)] dr \quad (14)$$

$$\eta_i = \frac{\bar{v}_{Ri}}{v_{Ri,s}} \quad (15)$$

The calculated error in balance closure for all the chemical species was below 7 % (reported to the left term in equation (14)). Note that this error is including both the accuracy of numerical integration of differential equations and the numerical error in calculation of the integrals appearing in the mass balance relation (14).

a) Isothermal pellet. Response to combined step changes in CO and H₂ concentrations

It is considered a catalyst pellet in stabilized isothermal regime corresponding to the operating parameters given in table 2. At a certain moment, it was performed a step change in CO and H₂ molar fractions (0.06 to 0.09 for CO and 0.803 to 0.773). The results of simulation are presented in figure 1A, in terms of methanol molar fraction evolution at different radial positions. The stabilization time was defined as time necessary for methanol molar fraction to achieve 99 % of its new steady state value (given that the methanol molar fraction had the slowest dynamics inside the catalyst pellet). A stabilization time of 3.9 s is required for the achievement of a stabilized regime (fig. 1).

The internal catalyst pellet effectiveness factor is defined as the ratio between the average reaction rate on the pellet volume (\bar{v}_{Ri}) to the reaction rate at the external surface of the pellet ($v_{Ri,s}$):

In order to evaluate the dynamics of the internal effectiveness factor, this was calculated considering the composition profiles inside the catalyst pellet at different moments of time, for several pellet diameters and the same unsteady process defined previously.

The calculated time evolutions of the effectiveness factors for reactions (1)-(3) are presented in figure 1C. The most important variation of the effectiveness factor is observed for reaction (2), due to the higher influence of CO concentration over the equilibrium of the water gas shift reaction.

b) Isothermal pellet. Response to a step change in surface temperature

In order to evaluate the catalyst pellet behavior in dynamic operating conditions typical for methanol synthesis in forced unsteady-state regime reactors, a catalyst pellet was considered in stabilized isothermal regime, the simulation being performed using the data given in table 2. At a certain moment, it was considered a step change in external surface temperature, from 533 to 523 K. The results of the simulation are presented in figure 2A, in terms of the evolutions of methanol molar fractions at different radial positions. As can be seen, a stabilization time of less than 2 s is required for the achievement of steady state regime after a step decrease of external surface temperature of 10 K.

In figure 2B and 2C there are represented the methanol profiles inside the catalyst particle and time evolutions of the effectiveness factors. As can be observed, the

Variable, symbol	Values and units
Temperature, T	533 K
Pressure, P	50 bar
External gas phase composition (molar fractions)	y _{CO} = 0.06; y _{CO2} = 0.0513; y _{CH3OH} = 0.0045; y _{H2} = 0.803; y _{H2O} = 0.001; y _{N2} = 0.0802
Catalyst pellet density	1950 kg m ⁻³
Catalyst pellet diameter, d _p	4.2 · 10 ⁻³ m
Catalyst pore radius, r _{por}	10 · 10 ⁻⁹ m
Catalyst void fraction, ε _p	0.5

Table 2
SIMULATION DATA

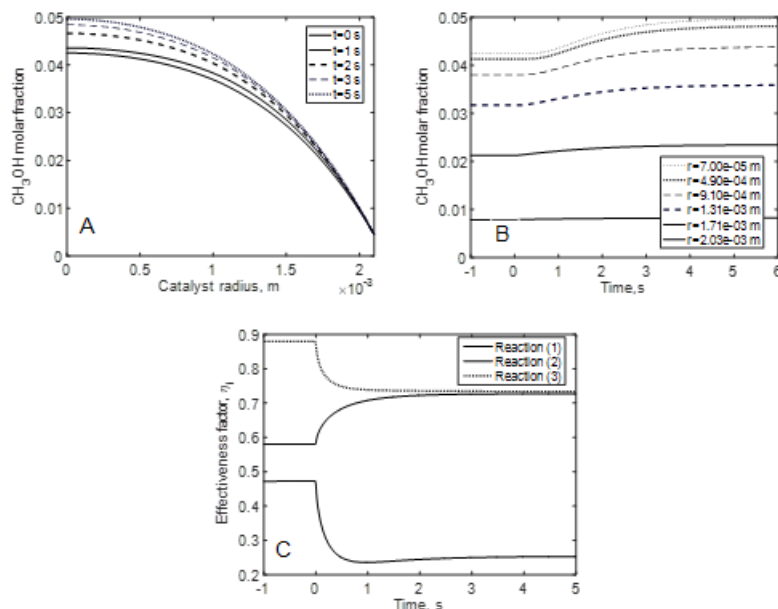


Fig. 1. The methanol molar fraction profiles inside the catalyst pellet (A), methanol molar fraction (B) and effectiveness factor (C) evolutions in time following a step change in CO and H₂ molar fraction at (T=533 K, P=50 bar; R_p=2.1 mm)

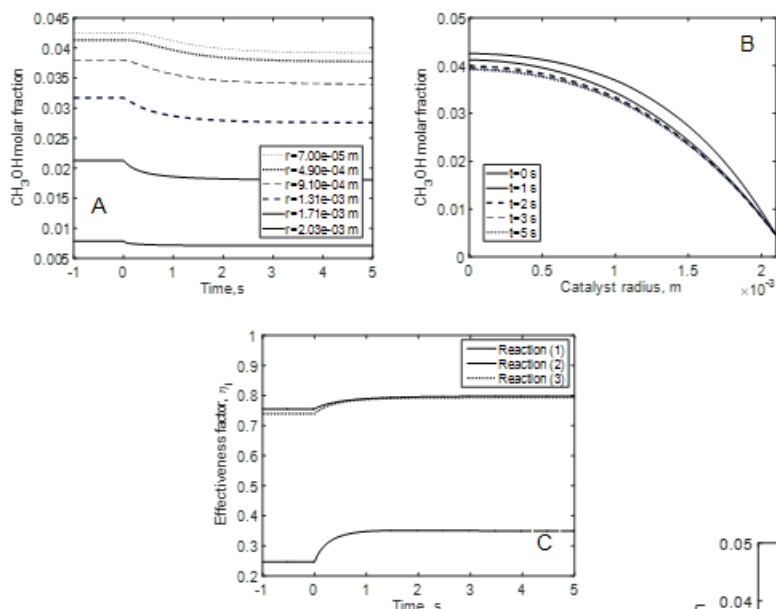


Fig. 2. The methanol molar fraction profiles (A), methanol molar fraction (B) and effectiveness factor (C) evolutions inside of catalyst pellet for a step change in surface temperature ($P=50$ bar; $R_p=2.1$ mm)

methanol concentration profiles are practically stabilized for time values above 2 s and, as expected, the effectiveness factor is increasing as result of a decrease in the reaction rates.

c) Isothermal pellet. Influence of the pellet size on the stabilization time

In order to evaluate the influence of the pellet size on stabilization time of the composition inside the pellet, it has been simulated the process during a step change in composition, similar with that described at the problem (a). At the initial moment is performed a step change in gas composition outside the pellet, from pure inert to the one given in table 2. The resulted time evolutions of methanol concentration in the center of the pellet (where the evolutions have the slowest dynamics), are represented in figure 3. The results presented in figure 3 are evidencing that the stabilization time increases with the pellet diameter, in the order $1.1 \text{ s} < 3.3 \text{ s} < 7.1 \text{ s} < 13 \text{ s} < 19.4 \text{ s}$ (from low to high diameters indicated in the figure's legend).

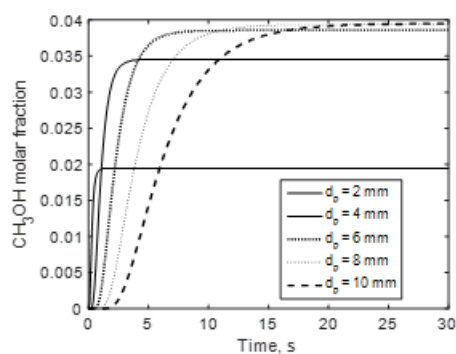


Fig. 3. Influence of the pellet size on the stabilization time, following a step change in external gas composition ($P=50$ bar, $T=533$ K)

d) Isothermal pellet. Influence of the reaction temperature on the stabilization time

In order to emphasize the influence of the temperature on the stabilization time, a catalyst pellet of 6 mm diameter have been considered, and its behavior was evaluated considering the unsteady process conditions defined for the problem (c). The calculated evolutions of the methanol concentration at the center of the pellet are presented in figure 4. As can be observed from this figure, the stabilization time is decreasing with the increase of the pellet temperature, in the order $9 \text{ s} > 8.2 \text{ s} > 7.9 \text{ s} > 7.3 \text{ s} > 7 \text{ s} > 6.1 \text{ s}$ (from lower to higher temperatures indicated in the figures legend) due to the temperature influence on the reaction kinetics.

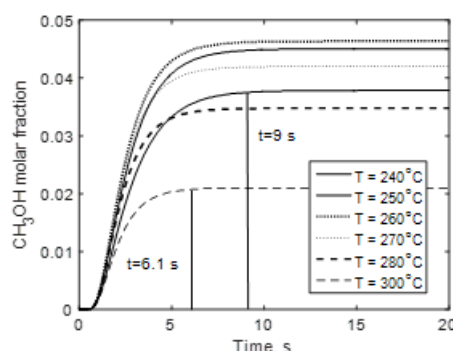


Fig. 4. Influence of the pellet size on the stabilization time ($d_p=6$ mm)

e) Non-isothermal pellet. Step change in the overall gas composition outside the pellet

A second category of simulation studies were performed considering the temperature variation inside the pellet. The mathematical model consists in balance equations (5) and (6), with the initial and boundary conditions [7].

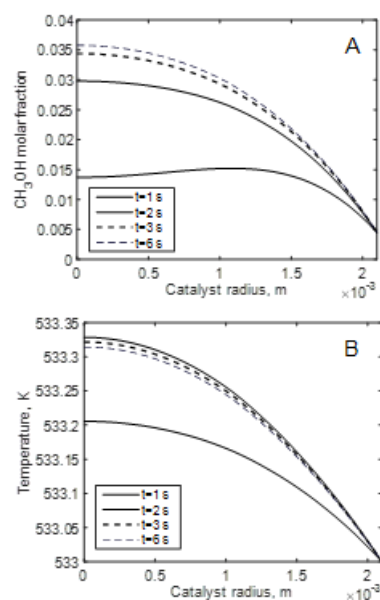


Fig. 5. Concentration and temperature evolutions inside the catalyst pellet, at different moments of time, following a step change in external gas composition (non-isothermal pellet; $P=50$ bar, $T=533$ K; $R_p=2.1$ mm)

At the initial moment, it is assumed the step change in gas composition outside the catalyst pellet, described for the problem (c). The results are presented in figure 5A in terms of methanol molar fractions at different time moments and figure 5B as the temperature profiles inside the catalyst pellet. In figure 6B there are presented the temperature evolutions at different radial positions inside the catalyst pellet. As observed, there is obtained a maximum temperature increase inside the pellet of approximately 0.3 K, i.e. a negligible temperature variation. The resulted stabilization times for both temperature and

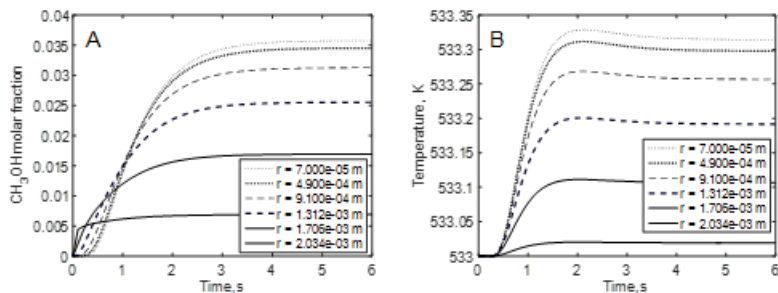


Fig. 6. Time evolutions of concentration and temperature inside the pellet, following a step change in external gas composition (non-isothermal pellet; $P=50$ bar, $T=533$ K; $R_p=2.1$ mm)

composition profiles are below 3 s. These results are demonstrating that the catalyst pellet in the methanol synthesis process can be considered as isothermal, at the temperature of the external surface.

f) Evaluation of the pellet effectiveness factor in unsteady-state regime

In order to evaluate the variations in the effectiveness factor of the catalyst pellet in unsteady operating conditions, there were considered the time variations of composition and temperature outside the pellet, during an unsteady operation time interval of 80 s, given in figure 7, typical for a catalyst bed operated in forced unsteady regime. The effectiveness factor was calculated using two methods: (i) from the variable internal composition and temperature profiles, obtained by solving the unsteady state pellet balance equations, progressively changing the surface concentration required in the boundary conditions

; (ii) considering that the process inside the pellet is instantaneously stabilized at the regime corresponding to the external surface composition and temperature, depicted in figure 7.

The results, presented in figure 8, are not evidencing significant differences between the effectiveness factor values calculated by the two methods. This is explained by the fast dynamics of the process inside the catalyst pellet, insuring the attainment of internal composition profiles close to the steady ones corresponding to the instant conditions at the pellet surface.

An interesting time variation is noted for the effectiveness factor of the reverse gas shift reaction (2), presented in figure 8C. This is featuring negative values at moments below 1 s and between 66 to 67 s of operation, indicating an effective occurrence of reaction (2) in the gas shift direction (formation of CO_2) on these intervals. This is illustrated more clearly in figure 9, where are

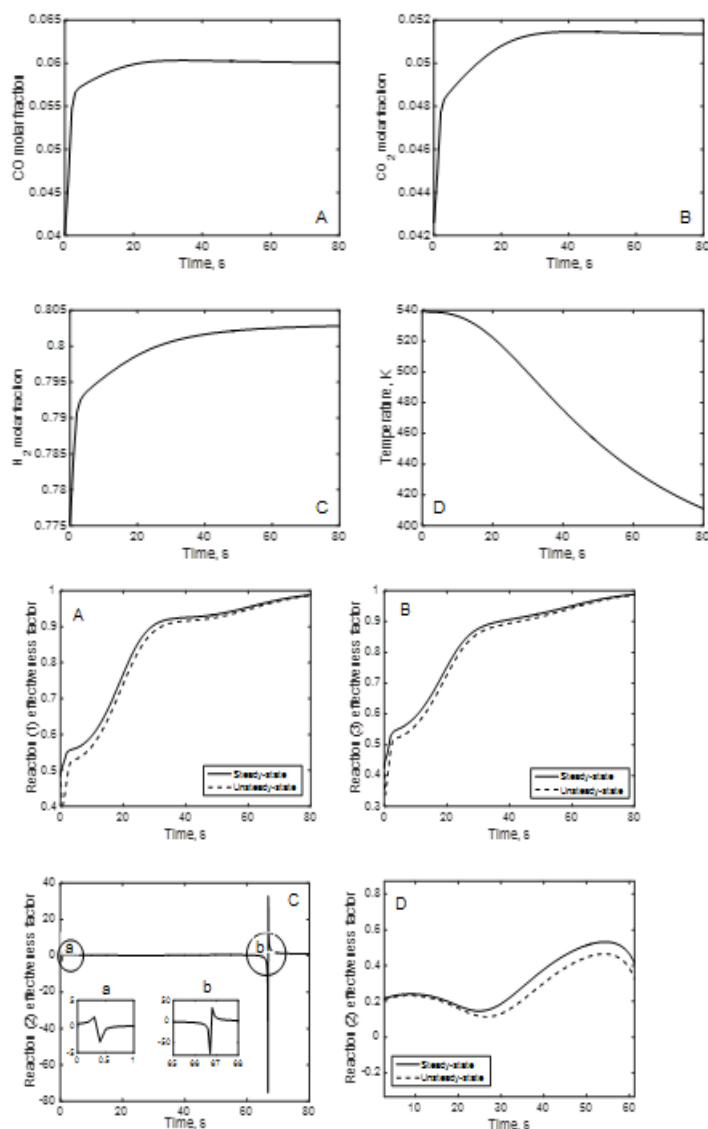


Fig. 8. Effectiveness factors evolutions for methanol synthesis reactions (1) - (3)

Fig. 7. The reactants mole fractions (A:CO, B:CO₂, C:H₂) and temperature (D) evolutions inside a packed bed reactor ($P=50$ bar).

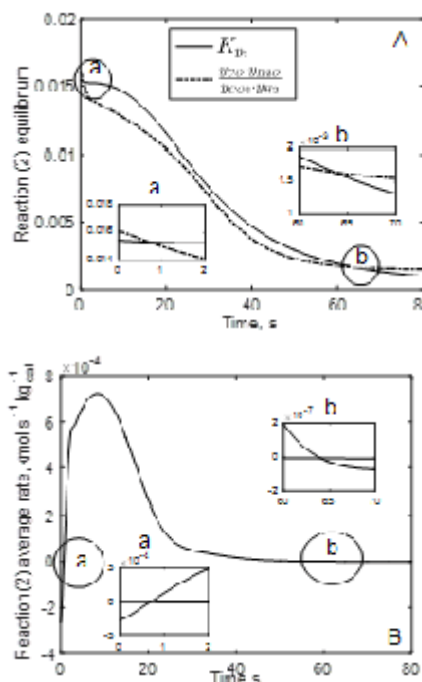


Fig. 9. Reaction (2) equilibrium (A) and average reaction rate evolutions

comparatively presented the actual and equilibrium states (A), as well as the time evolution of the rate of reaction (2). Similar effectiveness factor evolutions were reported by Elnashaie and Abashar [17], for water gas shift reaction taking place in the methane steam reforming process.

Conclusions

The paper described a process modelling and simulation for methanol synthesis process in unsteady state regime, at the level of the catalyst pellet. The model core is based on Wilke-Bosanquet diffusion-reaction model. The accuracy of the numerical calculations was checked by mass balances of chemical species over the simulated period of time. The results are evidencing a relatively fast dynamics of the process at the level of catalyst pellet, characterized by transition times of 3-4 s for typical industrial conditions. It was found that the process dynamics is strongly influenced by the size of catalyst pellet. The stabilization times for species concentrations are increasing with the decrease of diffusion coefficient value, being slightly longer for methanol. Another result regards the stabilization times for temperature inside the pellet, as response to step changes in external surface temperature (at constant external composition), which are shorter than those for composition, as response to external concentration steps. The results are also evidencing negligible temperature gradients inside the catalyst pellets (smaller than 0.5 K in typical working conditions), in accord with data reported in other studies. An interesting result is that the internal effectiveness factor calculated by the resolution of unsteady-state and steady state mass balance equations, for changes outside the pellet typical for forced unsteady regime, are close each other, this permitting a good approximation of effectiveness factor in unsteady regimes by the steady-state equations.

Acknowledgement: This work was supported by Project SOP HRD - PERFORM/159/1.5/S/138963.

References

1. BARTHOLOMEW C.H., FARRAUTO R.J., Fundamentals of industrial catalytic processes, Wiley, 2006
2. ROUT K.R., HILLESTAD M., JAKOBSEN H.A., Chem. Eng. Res. Des., **91**, 2013, p. 296
3. RASE H.F., Handbook of commercial catalysts heterogeneous catalysts, CRC Press, 2000
4. OLAH G.A., GOEPPERT A., PRAKASH G.K.S., Beyond oil and gas: the methanol economy, Wiley-VCH, 2009
5. STOICA I., BANU I., BOBARNAC I., BOZGA G., U.P.B. Sci. Bull., Series B, **77**, 2015, p. 133.
6. BOZGA G., BERCARU G., NAGY I., Rev. Chim. (Bucharest), **51**, 2000, p. 933.
7. NEOPHYTIDES S.G., FROMENT G.F., Ind. & Eng. Chem. Res., **31**, 1992, p. 1583.
8. VANDEN-BUSCHE K.M., NEOPHYTIDES S.N., ZOLOTARSKII I.A., FROMENT G.F., Chem. Eng. Sci., **48**, 1993, p. 3335.
9. VANDEN-BUSSCHE K.M., FROMENT G.F., Canad. J. Chem. Eng., **74**, 1996, p. 729.
10. SOLSVIK J., JAKOBSEN H.A., Chem. Eng. Sci., **66**, 2011, p. 1986.
11. LOMMERTS B.J., GRAAF G.H., BEENACKERS A.A.C.M., Chem. Eng. Sci., **55**, 2000, p. 5589.
12. GRAAF G.H., SCHOLTENS H., STAMHUIS E.J., BEENACKERS A.A.C.M., Chem. Eng. Sci., **45**, 1990, p. 773.
13. BOZGA G., MUNTEAN O., Reactoare chimice Vol. 2., Editura Tehnica, 2000.
14. POLING B.E., PRAUSNITZ J.M., O'CONNELL J.P., The properties of gases and liquids, McGraw-Hill, 2001
15. GRAAF G.H., STAMHUIS E.J., BEENACKERS A.A.C.M., Chem. Eng. Sci., **43**, 1988, p. 3185.
16. WOUWER A.V., SAUCEZ P., SCHIESSER W.E., Adaptive method of lines, CRC Press, 2001.
17. ELNASHAIE S.S.E.H., ABASHAR M.E.E., Chem. Eng. Process

Manuscript received: 1.07.2016